JOURNAL OF APPLIED ELECTROCHEMISTRY 26 (1996) 623–630

Characterization of Pt–Cu–Fe ternary electrocatalysts supported on carbon black

W. ROH, J. CHO, H. KIM

Department of Chemistry and Center for Molecular Catalysis, Seoul National University, San 56-1, Shinrim-dong, Kwanak-ku, Seoul 151-742, Korea

Received 10 March 1995; revised 31 October 1995

Ternary Pt–Cu–Fe alloy catalysts, useful for low temperature fuel cells, were prepared from aqueous media, followed by heat treatment at 900 °C for various heating periods. Supported metal crystallites were characterized with various techniques including XRD, XPS, TEM and ICP-AES. XRD patterns indicate that the lattice structure of platinum changes from a face-centred cubic to a contracted face-centred tetragonal structure as it forms an alloy. As the heating period increases, the extent of formation of an ordered alloy increases and the formation is completed in 2.5 h, as confirmed by the intensity of superlattice diffraction lines. The presence of different oxidation states is confirmed by XPS and the amount of higher oxidation state is reduced by heat-treatment, but there is no evidence of development of a new photoelectron peak or shift in binding energy by alloy formation. For the electrochemical reduction reaction of oxygen in fuel cell operation, ordered alloys have shown improved catalytic activity compared to platinum alone. After the stability test in hot phosphoric acid, the ordered structure is preserved even though a significant amount of transition metal is dissolved, and some increase in particle size in the heat-treated catalysts is observed.

1. Introduction

Platinum supported on carbon black has been commonly used for oxygen cathodes in phosphoric acid (PAFC) and solid membrane fuel cells. Recently, alloying supported platinum with other transition metals such as V, Cr, Co, Fe, Cu etc., has shown improved electrocatalytic activity towards oxygen reduction. The first binary alloy tested was Pt–V, but vanadium was leached out rapidly in phosphoric acid, leaving only platinum [1]. Landsman and Luczak [2] reported that Pt–Cr alloy was more active than Pt–V and Cr dissolved less than V. Jalan and Taylor [3] suggested that the catalytic enhancement of alloyed catalysts was related to the interatomic spacing of the atoms in binary alloys. They showed a linear relationship between specific activity and the nearest neighbour distance determined by X-ray diffraction. Pt–Cr alloy, which had the smallest nearest neighbour distance, thus exhibited the highest specific activity. Daube and coworkers [4] have investigated the role of Cr in a series of bulk Pt_x–Cr_{1-x} alloys ($0 \leq x \leq 1$). They concluded that Cr was leached out rapidly at anodic potentials, leaving a roughened platinum surface which gave higher catalytic activity towards oxygen reduction. Chung and coworkers [5] have suggested that partial alloying at moderately low temperature, followed by acid leaching of surface-enriched transition metal, is a good way of producing highly active alloy catalysts. They have shown that acid treatment (1 M H_2SO_4, at room temperature) of supported Pt–Fe catalyst alloyed at 750 °C gives a two-fold increase in the Pt surface area, doubling mass activity, when compared with the nontreated Pt–Fe alloy catalyst. It is not clear, however, that a similar roughening effect would occur as in the real operating conditions of a PAFC, that is, in the case of supported alloy catalysts with small particle size surrounded by hot phosphoric acid. Because the roughened surface may become rapidly smoothed by sintering, as predicted by Beard and Ross [6], the increase in Pt surface area will not occur. Watanabe *et al.* [7] have studied Pt–Co alloy systems in detail using the well defined crystallographic structures of alloy catalysts. They suggested that the ordered alloy exhibited a specific activity 1.35 times higher than the disordered alloy before corrosion testing (at 0.8 V and 205 °C in H_3PO_4 for 50 h), but has 0.73 times less activity after corrosion testing because of a higher degree of degradation of the ordered alloy.

In recent patents [8–17], it has been shown that the addition of two or more transition metals improves catalytic activity and stability. Luczak and Landsman [11] have demonstrated that Pt–Cr–Co alloy catalyst, which has an ordered structure, improves the specific activity and stability over nonordered alloys of similar composition. For an operating period of 9000 h at 200 °C in a subscale fuel cell test, the ordered alloy retained its ordered structure and chemical composition while nonordered alloys failed to demonstrate this physical and chemical stability under similar conditions. But fundamental characterization of these alloy catalysts had not been thoroughly

0021-891X

performed. Thus, there remains some controversy concerning the reasons for the increased activity towards electrochemical oxygen reduction by alloyed catalysts.

In the present work, we report on the preparation of a series of Pt–Cu–Fe ternary catalysts (atomic ratio, Pt:Cu:Fe = 2:1:1) for various heating periods at 900 °C and their characterization by various techniques, such as powder X-ray diffraction (XRD), X-ray photoelectron spectroscopy (XPS), transmission electron microscopy (TEM), and inductively coupled plasma–atomic emission spectroscopy (ICP–AES). Also, we report on the catalytic activity and stability of these catalysts for oxygen reduction in phosphoric acid to investigate the alloying effect.

2. Experimental details

2.1. *Preparation of alloy catalysts*

All alloy catalysts were prepared starting from commercially available carbon supported Pt catalyst (Johnson Matthey, 10 wt % Pt, about 120 $m^2 g^{-1}$ Pt). 1 g of Pt/C was dispersed in 25 ml of deionized water and ultrasonically stirred for 10 min. Appropriate amounts of 0.1 M solution of transition metal salts ($FeCl_2$, $CuCl_2$) were added to this suspension. The atomic ratio of Pt, Cu and Fe was adjusted to 2:1:1 in all resulting catalysts. The pH of the solution was adjusted to 8.0 by dropwise addition of 0.5 M NH_4OH and was ultrasonically blended for 20 min and stirred for 5 h. The suspension was filtered and the residue was dried at 100 °C for 2 h. Quantitative analysis of the loaded amount of metal was made by analysing the remaining metal ion concentration in the filtrate with an ICP–AES (Labtam). The dried catalysts were heat treated at 900 °C in a reducing atmosphere (10% H_2 and 90% N_2) and cooled to room temperature under flowing inert gas. The morphology of the catalyst was observed with a TEM (Joel).

2.2. *Stability test*

To determine the stability of the catalysts, 0.2 g of catalyst was dispersed in 20 ml of 100% H_3PO_4. The slurry was heated to 200 °C and maintained at this temperature for 5 h with continuous stirring in air. After being cooled to room temperature, the slurry was diluted with deionized water and filtered. The residue was rinsed extensively with deionized water and the amount of metal ions in the filtrate was analyzed with an ICP–AES, and the morphological change of the catalyst was observed by TEM.

2.3. *Activity test*

The electrode was composed of an electrocatalyst layer and a gas diffusion layer. The gas diffusion layer was prepared with carbon paper (0.1 mm thick, Toray) which was wet-proofed with FEP (copolymer of tetrafluoroethylene and hexafluoropropylenes, Mitsui) solution. A slurry made by mixing the catalyst and PTFE (30 wt %) was kneaded, rolled, and bonded to the carbon paper using an appropriate pressure, and heated at 340 °C for 1 h in air. The electrochemical reduction of oxygen was measured in a half cell apparatus. The reference electrode was a dynamic hydrogen electrode (DHE, 50 mV lower than NHE) and counter electrode was a large area platinum gauze. The measurement was carried out at 200 °C in 100% purified phosphoric acid as described elsewhere [18]. Polarization curves for oxygen reduction were obtained by potentiostatic method (Parc 173).

2.4. *X-ray diffraction (XRD)*

X-ray diffraction patterns of supported catalysts were obtained with a CN2115 diffractometer (Rigaku) with nickel-filtered CuK_α radiation. The X-ray gun was operated at 40 kV and 300 mA. Powder samples were mounted on glass slides.

2.5. *X-ray photoelectron spectroscopy (XPS)*

XPS spectra of supported catalysts were obtained using a VSW XPS/AES spectrometer. The spectrometer consisted of a monochromatic AlK_α (1486.6 eV) X-ray source and a hemispherical multichannel analyser. The X-ray source was operated at a power of 100 W (10 kV, 10 mA). The operating pressure of the main analysis chamber was below 10^{-9} torr. Absolute binding energies were referenced against the C 1s photoelectron peak (284.6 eV). XPS intensity ratios were calculated from the total integrated areas of the C 1s, Pt 4f, Cu 2p, and Fe 2p photoelectron peaks.

3. Results

3.1. *X-ray diffraction*

Powder X-ray diffraction analyses were performed to determine the crystal lattice structure of supported metal particles, order–disorder transformation, and to estimate the particle size of dispersed metal. Figure 1 shows XRD patterns of Pt alone catalyst and Pt–Cu–Fe ternary catalysts (denoted as PCF) which were heat-treated at 900 °C for various periods to investigate the change of crystal structure. The pattern from nonheat-treated catalyst (PCF(0), the number in parenthesis indicates the heating period in hours) shows no discrete peak, indicating that the size of particles is below 3 nm, and that it simply consists of the small particles of Pt and transition metals. The Pt alone crystal is identified as a face-centred cubic lattice structure. But in the case of heat-treated PCF catalysts, the crystal structure is transformed into a tetragonal lattice structure, which is confirmed by splitting of the (2 2 0) diffraction line near 69° (2θ). The extra lines which appear

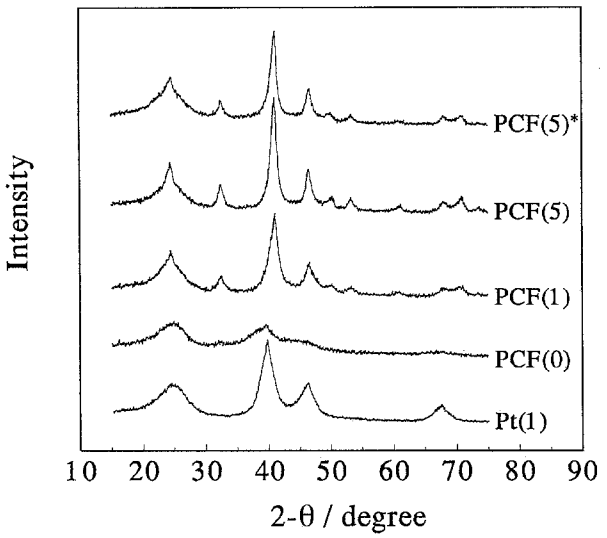

Fig. 1. X-ray diffraction patterns of Pt/C and Pt–Cu–Fe/C catalysts. The number in each sample name designates the heating period in hours at 900 °C. (*) after stability test.

in the patterns of PCF alloy are called superlattice lines, and their presence is a direct evidence that ordered alloy has formed [19].

The results of XRD analyses are summarized in Table 1. This also includes the results of the stability test. The lattice parameters of all catalysts are determined by least square extrapolation using (1 1 1), (2 0 0) and (2 2 0) diffraction lines. The lattice parameter values of ternary alloy catalysts decrease from the Pt value of $a = b = c = 392.4$ pm to $a = b = 389.1 - 390.6$ pm and $c = 362.1 - 365.6$ pm after heat-treatment at 900 °C, as alloy is formed. Upon alloy formation with transition metals, the lattice structure of Pt crystal changes from f.c.c. to contracted tetragonal structure. The duration of heating yields a small change in the lattice parameter. After the stability test in hot phosphoric acid, the lattice parameter of PCF(0) is almost the same as that of Pt. No dramatic change is observed in heat-treated catalysts, and diffraction peaks assigned to single phase Pt [7] are not detected, as shown in the top of Fig. 1, indicating that the alloy structures are almost completely maintained.

The average particle size of crystallites was calculated from the line broadening of (1 1 1) diffraction line using Scherrer's formula [20]. The instrumental broadening was corrected using silicon powder, whose particle size was large enough to eliminate any particle size broadening. The particle size grows gradually until a maximum is reached at 2.5 h, and no further increase is observed with prolonged heating. After the stability test, the average particle size of nonheat-treated catalyst (PCF(0)) significantly increases while those of heat-treated catalysts are almost unchanged. For example, the particle size of nonheat-treated Pt catalyst increases about seven times while that of heat-treated Pt catalyst is almost the same. Thus, we suggest that preheating a catalyst in a gas phase can prevent abrupt sintering in hot phosphoric acid.

The relative intensity of the superlattice line (1 1 0) to the fundamental line (1 1 1) indicates the extent of ordered alloy formation [19]. As the heating period increases, the ratio of the (1 1 0) to (1 1 1) peaks also increases, but there is almost no change in those of the PCF(2.5) and PCF(5) samples. This indicates that the formation of ordered alloy is complete in 2.5 h. Calculation of the order parameter indicates that the PCF(2.5) catalyst is ordered as PtM (M = Cu or Fe) alloy by about 94%. The intensity ratios of the (1 1 0) to (1 1 1) peaks decrease in all catalysts after the stability test. In the case of PCF(2.5) about 12% of the ordered alloy structure is destroyed. This indicates that even the ordered alloy is not perfectly stable in hot phosphoric acid.

3.2. *X-ray photoelectron spectroscopy*

XPS was employed for the qualitative and quantitative identification of various species on the surface of the supported alloy catalysts. Initially, a survey scan spectrum was obtained to identify the elements present in each sample. C 1s, Pt 4f, Cu 2p, and Fe 2p photoelectron spectra were then collected over sufficient time for analysis by curve fitting with an appropriate confidence level. Bulk Pt and Cu foil, whose surfaces were cleaned by Ar ion sputtering (30 min, 0.5 kV) were employed to determine the shape of the metallic Pt 4f and Cu 2p photoelectron spectra. Curve fitting was accomplished using the same method as described elsewhere [21].

Figure 2 shows the curve fitted Pt 4f spectra of

Table 1. XRD analysis of Pt/C and Pt–Cu–Fe/C catalysts before and after stability test in H_3PO_4 at 200 °C for 5 h

Catalysts	*Lattice parameter*/pm				*Particle size*/nm		(1 1 0)/(1 1 1) *Peak area ratio*/%	
	Before		*After*		*Before*	*After*	*Before*	*After*
	a	*c*	*a*	*c*				
PCF(0)	–	–	392.3	–	3.05	10.95	–	–
PCF(0.5)	390.6	364.6	389.7	365.4	5.71	6.61	13.6	10.4
PCF(1)	390.3	365.6	387.5	367.9	5.72	5.52	15.5	10.4
PCF(2.5)	389.1	362.1	389.9	363.4	7.95	8.19	21.2	11.8
PCF(5)	390.2	364.6	391.0	364.6	7.68	7.95	20.0	14.9
Pt(1)	392.4	–	392.9	–	4.16	4.16	–	–
Pt(0)	–	–	392.2	–	2.33	16.81	–	–

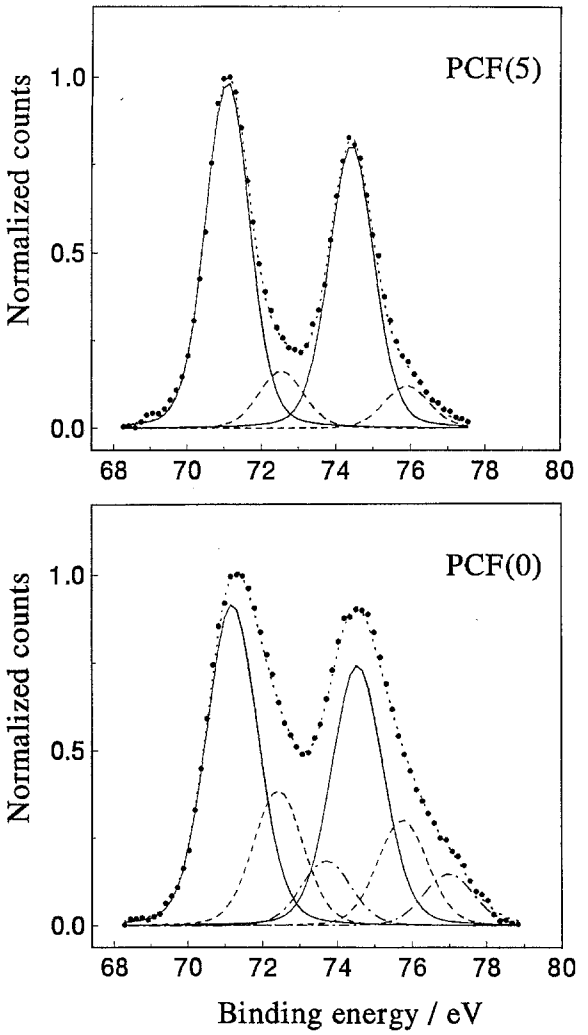

Fig. 2. Curve fitted XP spectra of Pt 4f region in Pt–Cu–Fe/C catalysts. PCF(0) shows three doublets and PCF(5) shows two doublets due to the presence of oxidized Pt species. Key: (●) background subtracted raw data, (. . . .) sum of curve fitted data.

nonheat-treated and 5 h heat-treated Pt–Cu–Fe catalysts. In the case of nonheat-treated catalyst, the curve fitted spectrum indicates the presence of metallic Pt and two other oxidation states (i.e., Pt(II) and Pt(IV)) based on the chemical shift of binding energies [22].

The results of curve fitted spectra from the Pt 4f and Cu $2p_{3/2}$ region are summarized in Table 2. The binding energies of the major elements in all Pt–Cu–Fe catalysts are slightly higher than those of sputtered metal foil because of the interaction between the metal and the carbon support containing oxygenated carbon functional groups [23]. The exact nature of the oxidized Pt species is not known because the O 1s signal cannot be quantitatively utilized to identify them because of the oxygenated functional groups on the carbon support. Upon heating to 900 °C, most of the oxidized Pt species are reduced, as expected, leaving a small amount of Pt(II) species. Thus, it is certain that these two minor Pt states are not related to the formation of an intermetallic phase with Cu or Fe. The duration of heating has little effect on the binding energy and on the relative amount of oxidized species.

Table 2. Observed binding energies and relative peak area from curve fitted Pt 4f and Cu $2p_{3/2}$ regions in Pt–Cu–Fe/C catalysts and sputtered metal foils

Catalyst	*Binding energy and relative peak area*		
	Pt $4f_{7/2}$ /eV	*Pt $4f_{5/2}$* /eV	*Cu $2p_{3/2}$* /eV
PCF(0)	71.2	74.6 (62.6%)	932.1 (58.8%)
	72.4	75.8 (25.2%)	934.0 (41.2%)
	73.7	79.0 (12.2%)	
PCF(1)	71.2	74.4 (86.4%)	932.0 (66.1%)
	72.5	75.9 (13.6%)	933.9 (33.9%)
PCF(5)	71.1	74.4 (86.2%)	932.0 (85.7%)
	72.5	75.9 (13.8%)	933.6 (14.3%)
Pt foil	70.6	74.0	
Cu foil			931.6

Figure 3 shows XP spectra from the Cu 2p region in Pt–Cu–Fe catalysts. Nonheat-treated samples show the $2p_{1/2}$–$2p_{3/2}$ spin-orbit doublet, accompanied by a shake-up peak at around 943 eV. Shake-up occurs when the valence electron is promoted to an unfilled higher energy level, and the presence of this satellite provides strong evidence of copper in the Cu(II) oxidation state [24]. As the sample is heated at

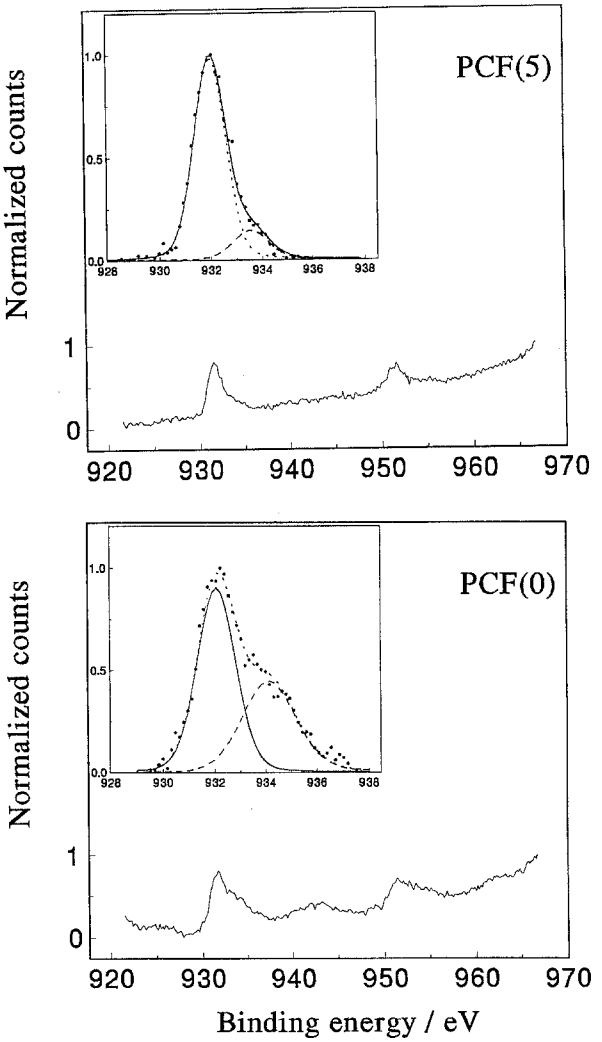

Fig. 3. Curve fitted XP spectra of Cu $2p_{3/2}$ region in Pt–Cu–Fe/C catalysts. Key: (●) background subtracted raw data, (- - - -) sum of curve fitted data.

Table 3. Atomic ratio calculated from C 1s, Pt 4f, and Cu $2p_{2/3}$ peaks from spectra of Pt–Cu–Fe/C catalysts before and after stability test

Catalyst	Atomic ratio			
	Pt/C		Cu/Pt	
	Before	After	Before	After
PCF(0)	0.011	0.0075	0.74	0.063
PCF(1)	0.011	0.011	1.0	0.071
PCF(5)	0.0071	0.011	0.60	0.13

Table 4. Activity for oxygen reduction measured at 0.9 V vs DHE, in 100% H_3PO_4 at 200 °C

Catalyst	Mass activity /A g^{-1}	Specific activity /μA cm^{-2}
Pt(1)	64	68
PCF(0)	28	21
PCF(0.5)	68	97
PCF(1)	73	104
PCF(2.5)	96	190
PCF(5)	76	145

900 °C, the size of the shake-up satellite diminishes gradually and almost disappears after 5 h of heating. This indicates that Cu(II) is reduced to metallic Cu or Cu(I) as a result of heat-treatment in a reducing atmosphere. These two species cannot be characterized by XPS since their binding energies are identical within 0.1 eV. Unfortunately, the XP spectra of the Fe 2p region are unsuitable for analysis or quantification of iron species because of large inelastic electron backgrounds. But judging from the broad peaks in the region of the Fe 2p spectra (708–725 eV), more than a few oxidized species may exist as mixed forms.

Table 3 shows atomic ratios calculated from C 1s, Pt 4f, and Cu $2p_{3/2}$ spectra. The atomic ratios were determined from the total integrated area of each peak whose X-ray satellites and background were subtracted by the Shirley method [25] with consideration of sensitivity factors [26]. The atomic ratio of platinum to carbon (Pt/C) can be used to determine the relative amount of surface platinum which is accessible for XPS detection and to estimate the dispersion of Pt on the carbon surface. The atomic ratio of Pt/C of nonheat-treated catalyst (PCF(0)) decreases by about 30% after the stability test, while those of heat-treated catalyst remains unchanged (PCF(1)) or even increases (PCF(5)).

It is evident from the XRD results that the particle size of nonheat-treated catalyst grows considerably with sintering, resulting in a decrease in Pt dispersion after the stability test, while that of heat-treated catalysts is unchanged. The atomic ratio of copper to platinum (Cu/Pt) for all catalysts is larger than the bulk composition ratio of 0.5, which indicates that copper must be concentrated on the surface of the carbon supports. After the stability test, Cu/Pt is reduced significantly because of the loss of copper in hot phosphoric acid. But the Cu/Pt loss of PCF(5) is smaller than for other catalysts. This is due to the highly ordered alloy, as in the PCF(5) sample, being protected from copper dissolution.

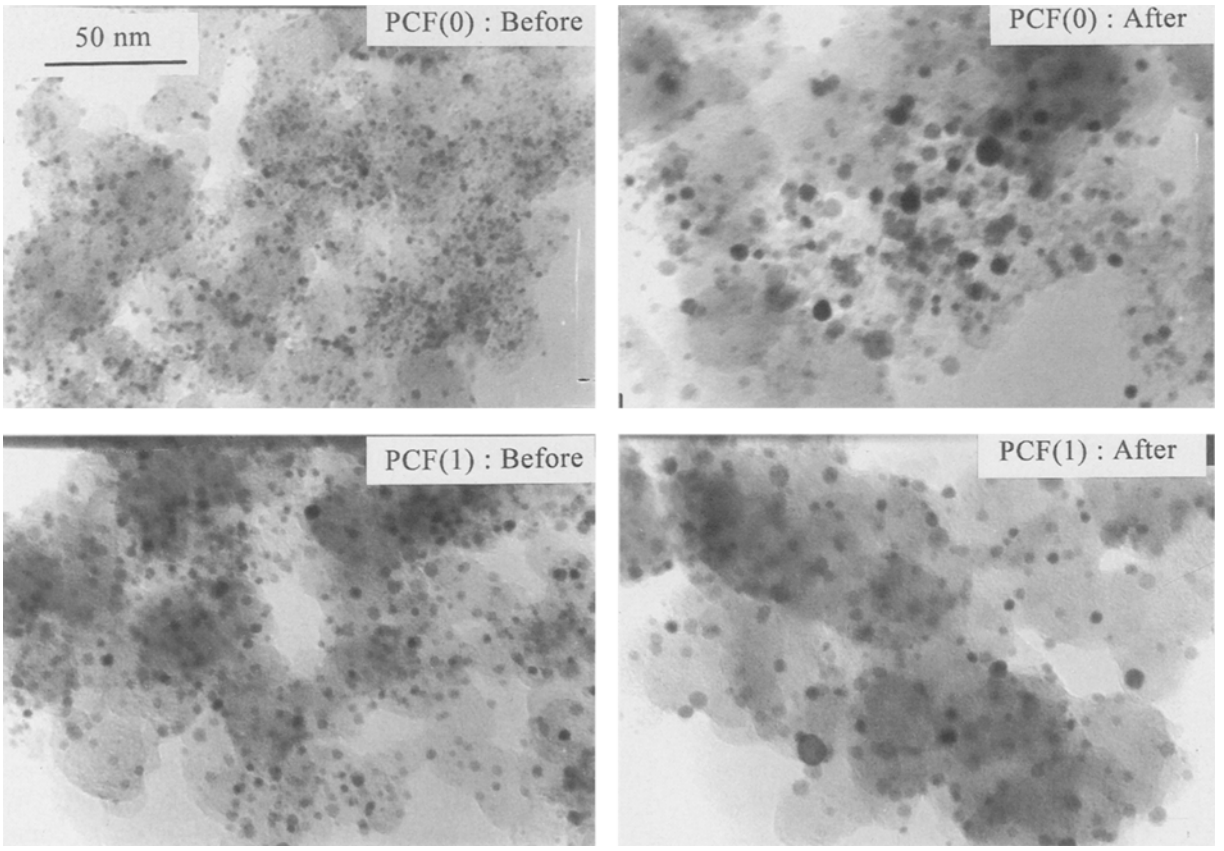

Fig. 4. TEM images of Pt–Cu–Fe/C catalysts before and after stability test in hot H_3PO_4 at 200 °C.

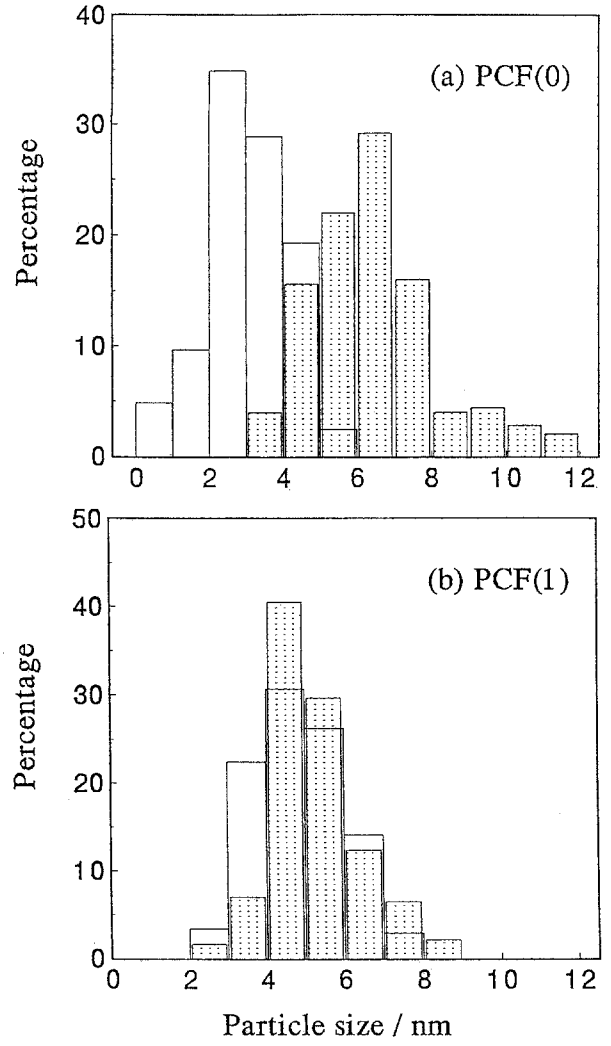

Fig. 5. Particle size distribution of supported metal species in Pt–Cu–Fe/C catalysts. Before stability test: unshaded bars; after stability test: shaded bars.

3.3. *Catalytic activity and stability*

Catalytic activity was measured to investigate the effect of alloying on the electrochemical reduction of oxygen. The results are summarized in Table 4. The activity of heat-treated Pt catalyst, which is used as the starting material for Pt–Cu–Fe catalysts, is included as a reference. The surface area of the metallic phase was calculated from X-ray diffraction line broadening. The activity of nonheat-treated catalyst (PCF(0)) is significantly lower than that of Pt catalyst while alloyed catalysts show slightly higher activity with a maximum in PCF(2.5). This agrees well with the results of XRD analysis, where the degree of alloy ordering increases with heating time and reaches a maximum at 2.5 h of heating. Thus, it can be suggested that, in the case of Pt–Cu–Fe ternary alloy catalyst, the formation of ordered alloy influences the enhancement of activity, though other effects, such as particle size or real surface area, could be involved.

Table 5. Amount of dissolution loss after stability test in 100% H_3PO_4 at 200 °C for 5 h

Catalyst	*Dissolution loss*/at %		
	Pt	*Cu*	*Fe*
Pt(1)	0.6		
PCF(0)	0.9	82.1	81.9
PCF(0.5)	0.8	70.4	56.1
PCF(1)	1.2	60.3	45.1
PCF(2.5)	0.5	61.4	33.6
PCF(5)	0.7	68.5	48.6

The stability test was performed to examine the dissolution loss of metals and to find any change of crystal structure in Pt–Cu–Fe catalysts in operational conditions of a phosphoric acid fuel cell. The morphological change of the catalysts was observed by TEM before and after the stability test, and the results are shown in Fig. 4. It is apparent that the particle size increases during the heat-treatment for alloying and the size distribution becomes broader after the stability test, as shown in Fig. 5. In the case of nonheat-treated catalyst, the particles are well dispersed on the carbon support with a narrow size distribution, but after the stability test, the average particle size increases abruptly, and abnormally large particles are produced. However, the size distribution of heat-treated catalyst is unchanged though abnormally small particles have disappeared. These results agree with the result of XRD that heat-treated catalysts are prevented from abrupt sintering of metal crystallites.

Quantitative analysis of the amount of lost metal was made by determining metal ions in the filtrate with an ICP–AES. The results are summarized in Table 5. Only a small amount of dissolution of Pt from all catalysts is observed in hot phosphoric acid, contrary to other work [10] which has claimed that the dissolution of Pt is reduced in alloyed catalysts. More than 80% of both Cu and Fe in nonheat-treated Pt–Cu–Fe catalyst is dissolved during the stability test. The dissolution loss of Cu and Fe metals, however, decreases in alloyed catalysts. Relating to the result of XRD analysis, less dissolution of transition metals is observed in ordered alloy. This tendency agrees well with other results obtained with Pt–Co alloy [6]. In the XRD analysis, alloy structure is preserved even though significant amounts of Cu and Fe are dissolved. It seems reasonable to believe that transition metals in unalloyed or small alloy crystallites are dissolved easily.

4. Discussion

In the course of preparing alloy catalysts, most of the copper and iron is deposited or adsorbed on the carbon support from solution, as confirmed by ICP–AES. Considering the solubility product and pH value of 8, the expected chemical species of both metal phases are hydroxides. Metal species may have considerable mobility and can contact each other at the elevated temperature of 900 °C. It is reasonable to expect that metal species in contact will form alloy clusters by the following reaction,

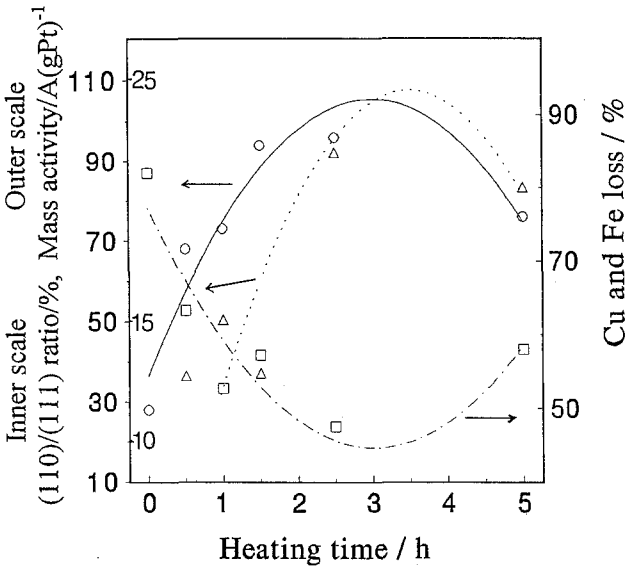

Fig. 6. Mass activity, (1 1 0)/(1 1 1) peak ratio and dissolution loss of total Cu and Fe plotted against heating time at 900 °C in Pt–Cu–Fe catalysts. Key: (○, ——) mass activity; (△, ...) (1 1 0/1 1 1) peak ratio; (□, – · – · –) total Cu and Fe loss.

suggested by Beard and Ross [6]:

$$2Pt + Cu(OH)_2 + Fe(OH)_2 + 2H_2 \longrightarrow Pt_2CuFe + 4H_2O$$

It is confirmed by XPS that a considerable amount of the higher oxidation states is reduced after heat-treatment. Since sufficient hydrogen is supplied and nitrogen flow removes the water vapour, the above reaction seems most probable during alloy formation in the case of 2:1:1 composition.

The crystal structure of clusters on the carbon support changes from a face-centred cubic to a contracted tetragonal structure as alloy forms during the heat-treatment. The formation of ordered alloy is almost complete in 2.5 h as confirmed by XRD results. Thus, heating more than 2.5 h at 900 °C only results in reduction of the active metal surface area.

The improved catalytic activity observed with Pt–Cu–Fe alloy catalysts in this study is related not only to the roughness effect, as suggested by Daube *et al.* [4], but also to the crystal structure. It is apparent that more ordered alloy exhibits larger mass activity; in addition, it is observed that transition metals in ordered alloy are less dissolved in phosphoric acid, as shown in Fig. 6.

It is known that the kinetics of oxygen reduction is influenced by the bond strength or coverage of oxygen molecules on the surface of an electrocatalyst [27]. Since the adsorptive properties of Pt must be changed by alloy formation with Cu and Fe, the enhanced activity with alloy catalysts seems to be related to these altered properties, in addition to the roughening effect and crystal structure, as mentioned earlier.

The stability of alloyed catalysts can be considered in two aspects. One is the reduction of metal surface area by sintering, and the other is the dissolution loss of metal under the operating conditions of a PAFC. Itoh *et al.* have reported that alloy catalyst is more resistant to sintering [10]. Based on the result of stability test, however, resistance to sintering seems not to be a result of the alloying effect because both alloy catalyst and heat-treated Pt catalyst show the same effect. The avoidance of sintering in heat-treated catalysts can be interpreted as follows. First, the average particle size of the catalyst increases to a certain extent during the heat-treatment, and these increased particles cannot move readily to collide with other particles. Second, as functional groups containing oxygen are detachable from carbon supports by heat-treatment, the micropores of the carbon support are exposed and, as a result, the surface area of the carbon support increases [21]. The collision probability decreases with this increased surface, and crystal particles in the catalysts are restrained from further growth in hot phosphoric acid.

As shown in Table 5, alloy catalysts suffer most from dissolution in phosphoric acid during the stability test. It is worth mentioning, however, that ordered catalysts show some stability compared to unordered ones. It is also interesting to note that the original crystal structure is preserved, even with such extensive loss of Fe and Cu.

Acknowledgements

This work was financially supported in part by the Han project (New Energy Development Project Component and Cell Technology Development for PAFC) through the Korea Institute of Energy Research (KIER), the Basic Science Research Institute project, Ministry of Education, Korea (BSRI 95-314) and by the Center for Molecular Catalysis and the Korean Science & Engineering Foundation. The authors also thank the Inter-University Center for Natural Research Facilities, Seoul National University for XPS experiments.

References

[1] V. M. Jalan, *US Patent 4 202 934* (1980).
[2] D.A. Landsman and F. J. Luczak, *US Patent 4 316 944* (1982).
[3] V. M. Jalan and E. J. Taylor, *J. Electrochem. Soc.* **130** (1983) 2299.
[4] K. Daube, M. Paffett, S. Gottesfeld and C. Campbell, *J. Vac. Sci. Technol A* **4** (1986) 1617.
[5] J. S. Chung, K. T. Kim, J. T. Hwang and Y. G. Kim, *J. Electrochem. Soc.* **140** (1993) 31.
[6] B. C. Beard and P. N. Ross, *ibid.* **137** (1990) 3368.
[7] M. Watanabe, K. Tsurumi, T. Mizukami, T. Nakamura and P. Stonehart, *ibid.* **141** (1994) 2659.
[8] J. S. Buchanan, G. A. Hards and S. J. Cooper, G.B. Patent, 2,242,203 (1991).
[9] F. J. Luczak, *US Patent 5 013 618* (1991).
[10] T. Itoh, S. Matsuzawa and K. Katoh, *US Patent 4 794 054* (1984).
[11] D. A. Landsman and F. J. Luczak, *US Patent 4 711 829* (1987).
[12] D. A. Landsman and F. J. Luczak, *US Patent 4 880 711* (1989).
[13] T. Itoh and K. Katoh, *US Patent 5 024 905* (1991).
[14] T. Itoh, K. Katoh and S. Kamitomai, *E. Patent 0 469 514 A2* (1991).
[15] L. Keck, J. Buchanan and G. A. Hards, *US Patent 5 068 161* (1991).
[16] K. Tsarumi, T. Nakamura and A. Sato, *US Patent 4 985 386* (1991).
[17] G. A. Capuano and A. Essalik, *US Patent 5 126 216* (1992).
[18] M. Watanabe, K. Makita, H. Usami and S. Motoo, *J. Electroanal. Chem.* **197** (1986) 195.
[19] B. D. Cullity, 'Elements of X-ray Diffraction', 2nd ed., Addison-Wesley, MA (1978) pp. 383–95.
[20] K. Kinoshita and P. Stonehart, 'Modern Aspects of Electrochemistry' vol 12 (edited by J. O'M. Bockris and B. E. Conway), Plenum, New York (1977) p. 235.
[21] J. B. Goodenough, A. Hamnett, B. J. Kennedy, R. Manoharan and S. A. Weeks, *Electrochim. Acta* **35** (1990) 199.
[22] K. S. Kim, N. Winograd and R. E. Davis, *J. Am. Chem. Soc.* **93** (1971) 6296.
[23] P. L. Antonucci, V. Alderucci, N. Giordano, D. L. Cocke and H. Kim, *J. Appl. Electrochem.* **24** (1994) 58.
[24] D. C. Frost, A. Ishitani and C. A. McDowell, *Mol. Phys.* **24** (1972) 861.
[25] D. A. Shirey, *Phys. Rev. B* **5** (1972) 4709.
[26] C. D. Wagner, L. E. Davis, M. V. Zeller, J. A. Taylor, R. M. Raymond and L. H. Gale, *Surf. Interface Anal.* **3** (1981) 211.
[27] K. Kinoshita, 'Electrochemical Oxygen Technology', Wiley-Interscience, New York (1992) p. 50.